[Article] www.whxb.pku.edu.cn

碳材料中多层次孔对负载铂电催化活性的影响

周建华 何建平* 计亚军 赵桂网 张传香 陈 秀 王 涛
(南京航空航天大学材料科学与技术学院, 南京 210016)

摘要: 分别以商用碳黑 XC-72、介孔碳 CMK-5 和含多层次孔的碳气凝胶 HCA 为载体, 微波法负载 Pt 纳米粒子, 在硫酸和甲醇溶液中进行循环伏安测试, 考察碳材料中多层次孔对其电催化活性的影响. 结果显示, Pt/HCA 电极表现出较高的峰电流(7.5 mA·cm^{-2})和电化学活性面积(128.0 m^2·g^{-1}). 这可能是因为碳气凝胶具有连续但非周期性的介孔结构, 有利于 Pt 纳米粒子的分散以及反应物质的传质.

关键词: 碳气凝胶; 多层次孔; 铂纳米粒子; 介孔; 电催化活性
中图分类号: O646

Influence of Hierarchical Porosity in Carbon Material on Electrocatalytic Property of Supported Pt Nanoparticles

ZHOU Jian-Hua HE Jian-Ping* JI Ya-Jun ZHAO Gui-Wang
ZHANG Chuan-Xiang CHEN Xiu WANG Tao
(*College of Material Science and Technology, Nanjing University of Aeronautics and Astronautics, Nanjing 210016, P. R. China*)

Abstract: The influence of hierarchical porosity on electrocatalytic property was investigated with Pt nanoparticles supported on three types of carbon materials, namely, commercial Vulcan XC-72, ordered mesoporous carbon CMK-5, and hierarchical carbon aerogel (HCA). The electrocatalytic activity of carbon supported Pt nanoparticles was verified by cyclic voltammetry in H_2SO_4 and CH_3OH solution. Pt/HCA presented superior performance with higher peak current (7.5 mA·cm^{-2}) and electrochemical active area (128.0 m^2·g^{-1}). This could be attributed to the carbon aerogel with continuous but nonperiodical mesopore structure, which facilitated dispersion of Pt nanoparticles and mass transport around reactants and products.

Key Words: Carbon aerogel; Hierarchical porosity; Pt nanoparticles; Mesopore; Electrocatalytic property

It is imperative to promote optimum activation of the catalyst component in the electro-oxidation of hydrogen and methanol, which would make fuel cell devices more efficient and more economic[1,2]. This is often done by getting well dispersed Pt nanoparticles on high-surface-area support while lowering the total amount of noble metal used and thereby increase Pt utilization[3–6].

Among the support materials for Pt nanoparticles, carbon black is normally used because of its appropriate electronic conductivity and surface area[7,8]. However, the diameter of the pores within the carbon particles is too small to provide access for fuel, electrolyte, and ions[9,10]. One advisable strategy to reduce performance degradation because of mass transport resistance is using an alternative carbon support with higher mesoporosity or marcroporosity[11,12].

One-dimensional periodic porosity has been functionally and aesthetically appealing. However, it is probably unsuitable for surface-based applications such as adsorption area and catalytic activity[13,14]. Hence, since carbon support has been found to possess strong influence on the accessibility of the active sites[15,16], more effort is still needed to seek out the optimum architecture of carbon support. Notably, carbon-silica composite aerogels

Received: December 3, 2007; Revised: January 31, 2008; Published on Web: March 26, 2008.
English edition available online at www.sciencedirect.com
*Corresponding author. Email: jianph@nuaa.edu.cn; Tel/Fax: +8625-52112626.
江苏省高新技术(BG2005009)和航空科学基金(2007ZF52061)资助项目

constructed with a continuous mesoporous network make it more expediently to ensure rapid mass transport of external reagents and offer electronic conduction paths to the catalyst. In this way, it became one of the preferred solutions to the hidden Pt problem, and the activity of supported electrocatalyst was enhanced by orders of magnitude[14,17].

In addition, the metal particles could hardly be adsorbed on the hydrophobic surface of supports. The actual loading of Pt nanoparticles is much less than the initial input, herein named as the lost Pt problem. It usually occurs during the process of reduction and subsequent treatments (e.g., rinse and dispersion)[18]. In the present work, we investigated the effects of surface area and mesopore percentage in three carbon supports on the Pt catalysts for electro-oxidation of hydrogen and methanol. The Pt nanoparticles were expected to have a high dispersion and excellent performance, which depended markedly on the pore character of carbon support.

1 Experimental

Commercial carbon black Vulcan XC-72 (Cabot), hierarchical carbon aerogel (HCA), and ordered mesoporous carbon CMK-5 were used as the support materials in the present work. Ordered mesoporous carbon CMK-5[1,19] was synthesized using SBA-15 as a hard template and furfuryl alcohol as a carbon source, followed by carbonization at 1073 K under N_2 atmosphere for 2 h. The synthesis of hierarchical carbon aerogel was based on the previously published works [20] with addition of Pluronic F127 (M_w=12600, PEO106PPO70PEO106, Sigma-Aldrich) as foamer. Briefly, 3.1 g resorcinol and 5.35 g formalin (37%(w)) were dissolved in 20 mL of magnesium hydroxide saturated solution under magnetic stirring for 30 min. Meanwhile, 0.1 g F127 was dissolved in 20 mL of ethanol to obtain transparent solution and then added to the initial solution. The mixture was stirred for another 1 h. After curing for 3 days at 363 K, the wet gels were immersed in acetone to exchange the water inside the pores and then dried at room temperature under ambient pressure. It was transformed into hierarchical carbon aerogel after further carbonization at 1073 K for 2 h under N_2 atmosphere. The catalysts with 20% (w) Pt were then prepared in a microwave oven (LG MG-5021MW1, 2450 MHz) at 700 W for 60 s[18].

The porous structures of the carbon supports were measured by N_2 adsorption and desorption isotherm using Micromeritics ASAP 2010 at 77 K. X-ray diffraction (XRD) patterns were recorded by a Bruker D8 ADVANCE diffractometer using Cu K_α radiation (λ=0.154056 nm). Transmission electron microscopy (TEM, FEI Tecnai G^2) operating at 200 kV was applied to characterize the morphology and particle distribution of the as-prepared catalysts. The electrical conductivity of the samples was determined by the four-point probe meter (Wentworth Laboratories probe station) at room temperature in conjunction with a multimeter (Keithley 6514 system electrometer).

An electrochemical interface (Solartron 1287) and a conventional three-electrode system were used to conduct voltammetry experiments at room temperature. A saturated calomel electrode (SCE) and a platinum foil were used as the reference electrode and the counter electrode, respectively. The working electrode was prepared according to our previous work[18]. The electrocatalytic activity was measured in 0.5 mol·L^{-1} H_2SO_4 between −0.22 V and 0.98 V at a scan rate of 20 mV·s^{-1} and in 2.0 mol·L^{-1} CH_3OH+1.0 mol·L^{-1} H_2SO_4 between 0 V and 1 V at the same scan rate. The chronoamperometry curves were investigated in the methanol system at 0.70 V.

2 Results and discussion

2.1 Porosity of different carbon supports

Three types of carbon supports were analyzed by the N_2 adsorption-desorption isotherms at 77 K, as given in Fig.1. It can be seen that Vulcan XC-72 has abundant micropores (<2 nm). The hierarchical carbon aerogel possesses a small quantity of micropores together with considerable mesopores of diameters approximately 6.0 nm. In addition, the isotherm of CMK-5 is of type IV with a pronounced H2-type hysteresis loop. It is indicated as an ordered mesostructure in CMK-5 with a narrow pore size distribution centered at 3.8 nm[1,19].

The calculated textural characteristics of different carbon supports are listed in Table 1. The data indicate that the hierarchical carbon aerogel consists of both mesopores and micropores like the conventional Vulcan XC-72 carbon. However, the percent-

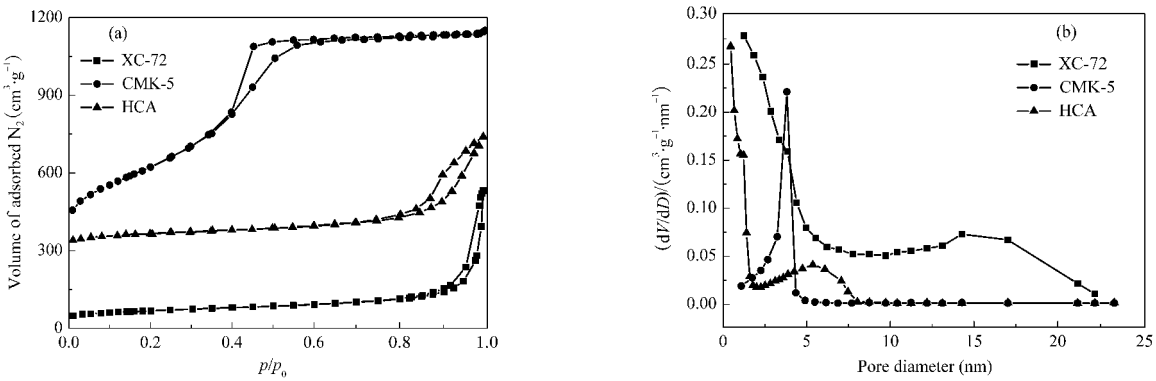

Fig.1 N_2 sorption isotherms (a) and pore size distribution curves (b) of the carbon supports

Isotherms for CMK-5 and HCA are offset vertically by 200 cm^3·g^{-1}.

Table 1 Textural characteristics of different carbon supports

Sample	S_{BET} ($m^2 \cdot g^{-1}$)	S_{micro} ($m^2 \cdot g^{-1}$)	V_{total} ($cm^3 \cdot g^{-1}$)	V_{meso} ($cm^3 \cdot g^{-1}$)	R_{meso}	Conductivity ($S \cdot m^{-1}$)
XC-72	231.2	87.7	0.82	0.51	62%	58.5
HCA	521.7	110.0	0.90	0.73	81%	73.9
CMK-5	1545.0	–	1.47	1.47	100%	37.6

S_{BET}: BET surface area; S_{micro}: micropore area; V_{total}: total pore volume; V_{meso}: mesopore volume; R_{meso} ($=V_{meso}/V_{total}$): mesoporosity

age of micropores is significantly less in the hierarchical carbon aerogel sample compared with that of Vulcan XC-72. It is suggested that the removal of F127 can yield the enhanced mesoporosity and the well-developed pore interconnectivity in hierarchical carbon aerogel. CMK-5 possesses dominant pores in the mesoporous range (<5 nm). Additionally, the electrical conductivities of these supports are comparable. Their support properties were also expected as the same order as the mesoporosity: CMK-5>hierarchical carbon aerogel>Vulcan XC-72.

2.2 Structural analysis of catalysts

XRD patterns of the Pt catalysts supported on different carbons are shown in Fig.2. For all the samples, the diffraction peaks at approximately 39°, 46°, 67°, and 81° are because of Pt(111), (200), (220), and (311) planes, which can be indexed to face-centered cubic phase[21]. The (220) diffraction peak was chosen to estimate average particle size using the Scherer equation[3] because there is no overlapping with other peaks. The average particle sizes are approximately 3.4 and 4.6 nm on Vulcan XC-72 and CMK-5, respectively. Additionally, the average particle size of Pt on hierarchical carbon aerogel support is the smallest (2.0 nm). Furthermore, the degree of crystallization[22] is evaluated by the peak intensity ratio of Pt(111) to graphite (002), as shown in Table 2. The value of Pt/HCA is the lowest, indicating the great electrochemical active area and superior catalytic performance.

From the TEM images in Fig.3, it is found that metal particles supported on hierarchical carbon aerogel are dispersed very uniformly at this magnification and have a narrow size distribution. All the Pt particles in Pt/HCA generally isolate each other. In comparison, there is conglomerating effect for the particles supported on both Vulcan XC-72 and CMK-5. The particles tend to aggregate into larger ones. This might have a disadvantage of lower active surface area exposed in the Pt/XC-72 and Pt/CMK-5 samples. In this way, homogenous dispersion and effective accessibility of Pt nanoparticles may be contributed to the large

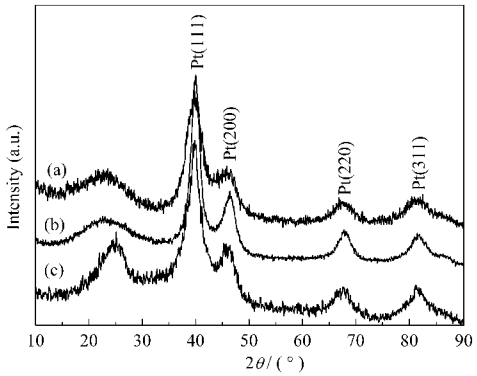

Fig.2 XRD patterns of Pt catalysts supported on Vulcan XC-72 (a), CMK-5 (b), and HCA (c)

Table 2 Calculated parameters of Pt nanoparticles from XRD and CV

Sample	Degree of crystallization (from XRD)	Oxidation peak current density ($mA \cdot cm^{-2}$)	Electrochemical active area ($m^2 \cdot g^{-1}$)
Pt/XC-72	2.13	4.2	81.8
Pt/CMK-5	2.18	5.8	69.8
Pt/HCA	1.56	7.5	128.0

pore space with continuous framework in carbon support, which would further enhance the electrocatalytic activity.

2.3 Electrocatalytic activity of catalysts

The stable and consistent CV curves after a few initial scans are shown in Fig.4 for the Pt catalysts in sulfuric acid. It can be clearly seen that all the curves show distinct hydrogen evolution peaks, which are characteristic of polycrystalline platinum, showing good activity of the Pt nanoparticles. For all the catalysts, the hydrogen region from −0.22 to 0.20 V (*vs* SCE) corresponds to the reductive adsorption of protons in the cathodic scan and the subsequent oxidation of the hydrogen adatoms in the anodic scan[23]. A smaller oxidation charge in this region for Pt/CMK-5, and especially for Pt/XC-72, implies a smaller electrochemical active area for these catalysts compared to Pt/HCA.

The electrochemical active area for Pt nanoparticles could be estimated from the integrated charge in the hydrogen adsorption region of the cyclic voltammograms, and normalizing with scan rate, Pt loading, and the charge value of 0.21 $mC \cdot cm^{-2}$ for Pt surface[24]. The calculated results of electrochemical parameters of Pt nanoparticles are listed in Table 2. With an equal amount of materials applied on the electrode, the electrochemical active area for Pt/HCA is 128.0 $m^2 \cdot g^{-1}$, while the value reduces to 64%

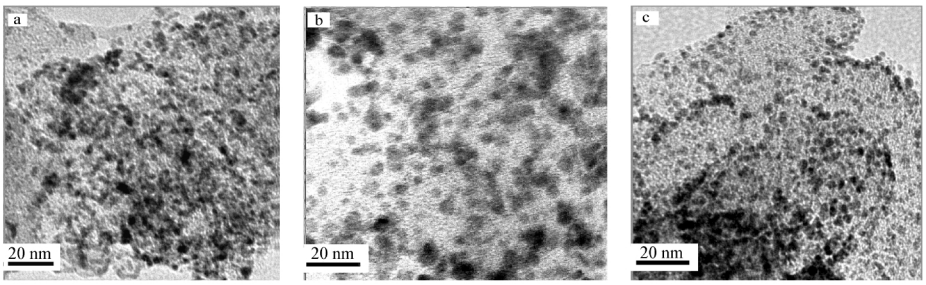

Fig.3 TEM images of Pt catalysts supported on Vulcan XC-72 (a), CMK-5 (b), and HCA (c)

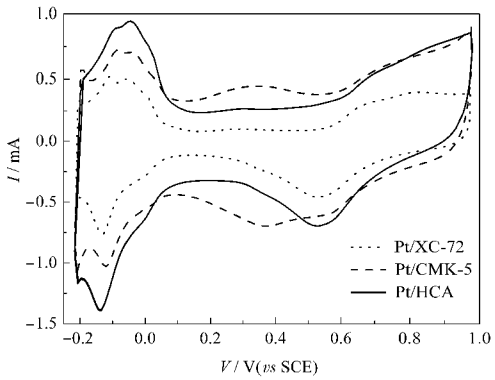

Fig.4 Cyclic voltammograms of ink electrodes in 0.5 mol·L^{-1} H_2SO_4 solution

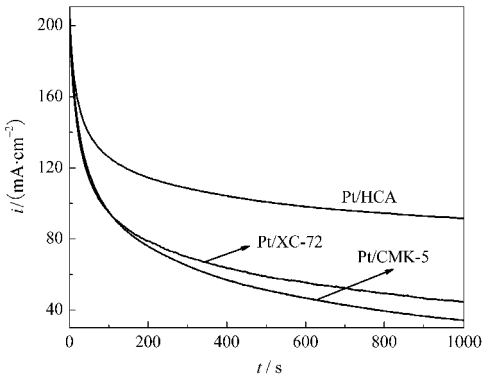

Fig.6 Chronoamperometry of ink electrodes in 2.0 mol·L^{-1} CH_3OH+1.0 mol·L^{-1} H_2SO_4 solution at 0.70 V

for Pt/XC-72 (81.8 $m^2 \cdot g^{-1}$). Besides, since the base line was taken by extrapolation of the double-layer region, which was mostly depended on the large mesopores, the Pt/CMK-5 gives the lowest value (69.8 $m^2 \cdot g^{-1}$), despite its little higher current than Pt/XC-72.

A carbon black, such as Vulcan XC-72, has been most frequently used as a support for electrocatalysts because it is inexpensive and has good corrosion resistance[8,9]. However, the presence of a significant amount of microporosity leads to a poor utilization of the Pt particles because the catalyst particles present in the micropores will not be accessible to the electrolyte for active sites[25]. In contrast, for a comparable metal particle size, ordered mesoporous carbon with higher surface area and larger amount of mesoporosity is expected to provide a high dispersion of Pt nanoparticles and high mass transport speed, and thus have a better electrocatalytic activity for hydrogen oxidation in acid solution. Unfortunately, the periodic mesopores in CMK-5 produced the largest double-layer capacitance at the same time[26], thus, the calculated activity for Pt/CMK-5 was weakened because of the rise of the base line. In view of the periodic porosity with one-dimensional channels, any internal blockage may make all flow and transport although the structure is limited[13,14]. Unlike the carbon using template synthesis, the pores in carbon aerogel are nonperiodical, representing mesopore space by slightly overlapping spheres in a continuous network[16,20], and may effectively offer transport routes around reactants and products. Hence, it is not surprising that Pt nanoparticles supported on hierarchical carbon aerogel present the best performance with the highest oxidation peak current density of the hydrogen adatoms (7.5 mA·cm^{-2}). The hierarchical, interconnected but nonperiodical pore structure on the mesoscale of carbon aerogel could make it be more suitable for the support in catalytic reaction, in agreement with the proposal of the novel catalytic nanoarchitecture[14].

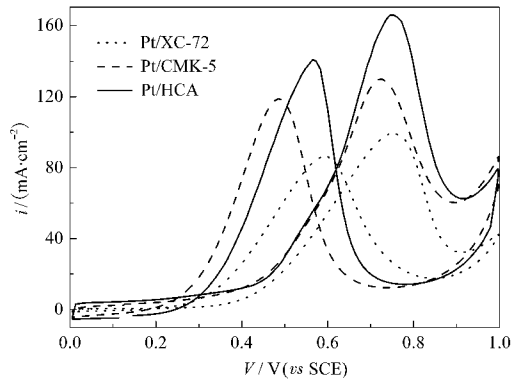

Fig.5 Cyclic voltammograms of ink electrodes in 2.0 mol·L^{-1} CH_3OH+1.0 mol·L^{-1} H_2SO_4 solution

It can be further proved in the electrolyte of 2 mol·L^{-1} methanol mixed with 1 mol·L^{-1} H_2SO_4 solution (Fig.5). The efficiencies of the specimens on methanol oxidation were compared in items of forward peak current density[27]. Pt/HCA displays a characteristic voltammogram with a relatively high value of the forward peak current density. For all the specimens, the CO desorption peak current densities during the reverse scan were significantly lower than their forward values, implying that all the catalysts indeed effectively suppress the adsorption of CO on the Pt surface.

Another important evaluation of catalytic performance is the stability at methanol oxidation potential. The current–time curves at 0.70 V are given in Fig.6. All the catalysts show a slight decay because of adsorbed reaction intermediates during the methanol electro-oxidation[28]. Pt/CMK-5 responds the same current as Pt/XC-72, however, it falls more rapidly after 200 s. Pt/HCA displays a gentle slope, indicating more resistant to poisoning by the reaction intermediates than the others. Furthermore, Pt/HCA gives superior performance with the highest current response.

3 Conclusions

Three types of carbon materials were loaded with Pt nanoparticles through the microwave irradiation method. On the carbon aerogel support, the Pt particles were dispersed very uniformly and had a narrow size distribution. Moreover, as a carbon aerogel support with the hierarchical, continuous but nonperiodical pore structure on the mesoscale offers transport routes around reactants and products, Pt/HCA presented the best performance with the highest peak current and stability. In contrast, both the periodic porosity with one-dimensional channels in CMK-5 and dominant micropores in Vulcan XC-72 would limit transport

from fuel to the anchorages of active Pt nanoparticles, which displayed inferior performance in acid and methanol.

References

1 Joo, S. H.; Choi, S. J.; Oh, I.; Kwak, J.; Liu, Z.; Terasaki, O.; Ryoo, R. *Nature*, **2001, 412**: 169

2 Tang, H.; Chen, J. H.; Wang, M. Y.; Nie, L. H.; Kuang, Y. F.; Yao, S. Z. *Appl. Catal. A*, **2004, 275**: 43

3 Liang, Y. M.; Zhang, H. M.; Yi, B. L.; Zhang, Z. H.; Tan, Z. C. *Carbon*, **2005, 43**: 3144

4 Hou, Z.; Yi, B.; Yu, H.; Lin, Z.; Zhang, H. *J. Power Sources*, **2003, 123**: 116

5 Zhou, W. J.; Zhou, Z. H.; Song, S. Q.; Li, W. Z.; Sun, G. Q.; Tsiakaras, P.; Xin, Q. *Appl. Catal. B*, **2003, 46**: 273

6 Coker, E. N.; Steen, W. A.; Miller, J. T.; Kropf, A. J.; Miller, J. E. *Micropor. Mesopor. Mater.*, **2007, 101**: 440

7 Shao, Y. Y.; Yin, G. P.; Zhang, J.; Gao, Y. Z. *Electrochim. Acta*, **2006, 51**: 5853

8 Wikander, K.; Ekstrom, H.; Palmqvist, A. E. C.; Lundblad, A.; Holmberg, K.; Lindbergh, G. *Fuel Cells*, **2006, 6**: 21

9 Roen, L. M.; Paik, C. H.; Jarvic, T. D. *Electrochem. Solid-State Lett.*, **2004, 7**: A19

10 Oskam, G.; Searson, P. C. *J. Phys. Chem. B,* **1998, 102**: 2464

11 Du, H. D.; Li, B. H.; Kang, F. Y.; Fu, R. W.; Zeng, Y. Q. *Carbon*, **2007, 45**: 429

12 Calvillo, L.; Lázaro, M. J.; García-Bordejé, E.; Moliner, R.; Cabot, P. L.; Esparbé, I.; Pastor, E.; Quintana, J. J. *J. Power Sources*, **2007, 169**: 59

13 Antonietti, M.; Ozin, G. A. *Chem. Eur. J.*, **2004, 10**: 28

14 Rolison, D. R. *Science*, **2003, 299**: 1698

15 Rao, V.; Simonov, P. A.; Savinova, E. R.; Plaksin, G. V.; Cherepanova, S. V.; Kryukova, G. N.; Stimming, U. *J. Power Sources*, **2005, 145**: 178

16 Du, H. D.; Gan, L.; Li, B. H.; Wu, P.; Qiu, Y. L.; Kang, F. Y.; Fu, R. W.; Zeng, Y. Q. *J. Phys. Chem. C*, **2007, 111**: 2040

17 Anderson, M. L.; Stroud, R. M.; Rolison, D. R. *Nano Lett.*, **2002, 2**: 235

18 Zhou, J. H.; He, J. P.; Ji, Y. J.; Dang, W. J.; Liu, X. L.; Zhao, G. W.; Zhang, C. X.; Zhao, J. S.; Fu, Q. B.; Hu, H. P. *Electrochim. Acta*, **2007, 52**: 4691

19 Dang, W. J.; He, J. P.; Zhou, J. H.; Ji, Y. J.; Liu, X. L.; Mei, T. Q.; Li, H. L. *Acta Phys. -Chim. Sin.*, **2007, 23**: 1085 [党王娟, 何建平, 周建华, 计亚军, 刘晓磊, 梅天庆, 力虎林. 物理化学学报, **2007, 23**: 1085]

20 Li, W. C.; Lu, A. H.; Schüth, F. *Chem. Mater.*, **2005, 17**: 3620

21 Boxall, D. L.; Lukehart, C. M. *Chem. Mater.*, **2001, 13**: 806

22 Wang, Y. E.; Tang, Y. W.; Zhou, Y. M.; Gao, Y.; Liu, C. P.; Lu, T. H. *Chem. J. Chin. Univ.*, **2007, 28**: 743 [王彦恩, 唐亚文, 周益明, 高 颖, 刘长鹏, 陆天虹. 高等学校化学学报, **2007, 28**: 743]

23 Papageorgopoulos, D. C.; de Bruijn, F. A. *J. Electrochem. Soc.*, **2002, 149**: A140

24 Li, W. Z.; Zhou, W. J.; Li, H. Q.; Zhou, Z. H.; Zhou, B.; Sun, G. Q.; Xin, Q. *Electrochim. Acta*, **2004, 49**: 1045

25 Raghuveer, V.; Manthiram, A. *J. Electrochem. Soc.*, **2005, 152**: A1504

26 Ding, J.; Chan, K. Y.; Ren, J. W.; Xiao, F. S. *Electrochim. Acta*, **2005, 50**: 3131

27 Tsai, M. C.; Yeh, T. K.; Tsai, C. H. *Electrochem. Commun.*, **2006, 8**: 1445

28 Shen, P. K.; Xu, C. W. *Electrochem. Commun.*, **2006, 8**: 184